JOURNAL OF AGRICULTURAL AND FOOD CHEMISTRY

Structural Ripening-Related Changes of the Arabinan-Rich Pectic Polysaccharides from Olive Pulp Cell Walls

SUSANA M. CARDOSO,*,†,‡ JOSÉ A. FERREIRA,‡ ISABEL MAFRA,‡,§ ARTUR M. S. SILVA,‡ AND MANUEL A. COIMBRA‡

Escola Superior Agrária, Instituto Politécnico de Bragança, Campus de Santa Apolónia, 5301-855 Bragança, Portugal, Departamento de Química, Universidade de Aveiro, 3810-193 Aveiro, Portugal, and REQUIMTE—Serviço de Bromatologia, Faculdade de Farmácia, Universidade do Porto, Rua Aníbal Cunha 164, 4099-030 Porto, Portugal

In this study, the structural features and ripening-related changes that occur in the arabinan-rich pectic polysaccharides highly enmeshed in the cellulosic matrix of the olive pulp fruit were evaluated. These pectic polysaccharides, obtained from two consecutive harvests at green, cherry, and black ripening stages, account for 11−19% of the total pectic polysaccharides found in the olive pulp cell walls and were previously shown to occur as calcium chelating dimers. On the basis of the ^{13}C NMR, (^{1}H, ^{13}C) *g*HSQC, 2D COSYPR, and (^{1}H,^{13}C) *g*HMBC carbon and proton resonances of the variously linked arabinosyl residues, we propose a tentative structure. This structure is particularly characterized by T-β-Ara*f* (1→5)-linked to (1→3,5)-Ara*f* residues and by the occurrence of branched and linear blocks in the arabinan backbone. Methylation analysis showed that these pectic polysaccharides of black olives have more arabinan side chains, which were shorter (less (1→5)-Ara*f*), highly branched (more (1→3,5)-Ara*f*), and with shorter side chains (fewer (1→3)-Ara*f*) than those of green and cherry olives. Quantitative ^{13}C NMR data indicated that these modifications involved the disappearance of the characteristic terminally linked β-Ara*f* residue of the arabinans. This odd feature can be used as a diagnostic tool in the evaluation of the stage of ripening of this fruit, as well as a marker for the presence of olive pulp in matrices containing pectic polysaccharides samples.

KEYWORDS: ***Olea europaea*** **L.; Douro variety; ripening; structure; methylation analysis; NMR.**

INTRODUCTION

Olive fruits are the raw material for a number of products, particularly olive oil and table olives. Olives are picked late in the Autumn or Winter, depending on the variety and on the desired characteristics of the final product. For table olive production, particularly for black oxidized processing, the olives harvested at different stages of ripening, i.e., green, cherry, and for certain varieties, black, are generally used. At these ripening stages, olives have distinct textures (*1*), which are greatly determined by structural changes in the cell wall pectic polysaccharides. In general, ripening originates an increase in the relative amount of arabinose in the pectic polysaccharides and an increase in their solubilization (*1*−*5*). These changes in the pectic polysaccharides might be related to the activity of cell wall degrading enzymes (*6*) and/or to the biosynthesis of new polysaccharides (*2*).

The arabinan-rich pectic polysaccharides represent one-third of the olive pulp cell walls (*7*). Their structure consists of a (1→4)-linked α-D-galacturonic acid (GalA) backbone that is interrupted in places by single residues of 2-*O*-linked-α-L-rhamnopyranose. Some of the Rha*p* residues are substituted at C-4 with L-arabinosyl and D-galactosyl residues as side chains. In olive pulp, the pectic L-arabinose side chains have a main structure of (1→5)-α-linked L-arabinofuranose units, substituted at *O*-3 (*7*, *8*), and are characterized by a T-β-Ara*f* linked at *O*-5 (*8*).

The sequential extraction of pectic polysaccharides from olive, as from many plant cell walls, implies the use of strong chelating agents such as CDTA or imidazole to remove Ca^{2+}-linked pectic polysaccharides. The polysaccharides in these extracts correspond, in the case of olive pulp (*1*, *2*, *7*), as well as in other fruits such as apple (*9*), to less than 50% of the total cell wall pectic polysaccharides. Further extraction of pectic polysaccharides can be obtained by mild de-esterification of plant cell walls with aqueous dilute carbonate solutions and by treatments with stronger alkali solutions of 0.5, 1, and 4 M KOH (*10*, *11*). After these extractions, the final cellulosic residue (CR) still contains considerable amounts of arabinan-rich pectic polysaccharides (*2*), which are highly entrapped in the cellulosic matrix. To the best our knowledge, the unique study regarding the pectic polysaccharides highly enmeshed in the cellulosic residue was

* Corresponding author. Tel: +351 273 303279. Fax: +351 273 325405. E-mail: scardoso@ipb.pt.
† Instituto Politécnico de Bragança.
‡ Universidade de Aveiro.
§ Universidade do Porto.

10.1021/jf070769w CCC: $37.00
Published on Web 07/21/2007

described by Ferreira et al. (*12*). These pectic polysaccharides were there obtained after neutralization and dialysis of the cellulosic residue of the olive pulp of two consecutive harvests at green, cherry, and black ripening stages. For the two harvests and the three stages of ripening, the arabinan-rich pectic fraction represented 3.4−4.8% of the cell wall material. Their powder X-ray diffraction analysis highlighted Ca^{2+}−pectic polysaccharide crystalline structures in the amorphous carbohydrate network, showing that these polysaccharides occurred in the olive pulp cell walls as calcium−GalA bridged macrodimers.

The aim of this work is to further characterize the pectic polysaccharides deeply enmeshed in the cell walls. The main structural features of the pectic polysaccharides from green olives will be highlighted by 1D and 2D NMR spectroscopy. Also, the structural ripening-related changes occurring in these pectic polysaccharides will be described on the basis of methylation and quantitative ^{13}C NMR data.

MATERIALS AND METHODS

Samples. Olive fruits (*Olea europaea* L. cv 'Negrinha do Douro') with an average length of 2.0 cm and a diameter of 1.2 cm were provided by Maçarico Lda, Praia de Mira, Portugal, at different stages of ripening: mature green (2.1 and 2.9 g pulp/fruit), changing color (cherry, 2.3 and 3.2 g pulp/fruit), and mature black (3.2 and 3.9 g pulp/fruit) for harvests of 1997 and 1998, respectively (*2*).

Preparation and Isolation of the Arabinan-Pectic Material. The cell wall material (CWM) from olives was prepared as described by Mafra et al. (*1*), and further used to obtain the arabinan-rich pectic polysaccharides, as previously described by Ferreira et al. (*12*). Briefly, the CWM was extracted with imidazole, carbonate, and KOH aqueous solutions (*1*, *2*), and the resultant cellulosic residue was suspended in water, acidified (pH 5−6) with glacial acetic acid, and dialyzed against distilled water. The supernatant from the dialysis of the cellulosic residue (sn-CR) was collected separately from the residue, by centrifugation and filtration, and the sn-CR fraction was then concentrated under reduced pressure, frozen under liquid nitrogen, and freeze-dried. For the two harvests and the three stages of ripening, the sn-CR fractions represented 3.4−4.8% of the cell wall material (*12*) and had a sugar content of 64−79%, composed of Ara (53−71 mol %), GalA (17−38 mol %), and minor amounts of Gal (4−8 mol %), Rha (1−4 mol %), Xyl (1−2 mol %), and Glc (1 mol %). These arabinan-rich pectic polysaccharides, highly entrapped in the cell walls, accounted for 11−19% of the total pectic polysaccharides found in the olive pulp cell walls of the fruits collected in the 2 years and in the three stages of ripening.

Methylation Analysis. The sn-CR polysaccharides were activated with powdered NaOH and methylated with CH_3I (*13*, *14*) as described by Coimbra et al. (*10*). The methylated material was dissolved in 1:1 v/v $CHCl_3$:MeOH, and the solution was dialyzed against 50% EtOH, evaporated, and freeze-dried. The methylated polysaccharides were hydrolyzed with TFA at 121 °C for 1 h, reduced by $NaBD_4$, and acetylated in the presence of acetic anhydride and 1-methylimidazole. The partially methylated alditol acetates were analyzed by GC-FID on an OV-1 capillary column (30 m length, 0.32 mm internal diameter, and 0.25 μm film thickness), and characterized by GC/MS. The samples were injected in splitless mode (time of splitless 0.75 min), with the injector and detector operating at 210 and 220 °C, respectively, using the following temperature program: 55 °C for 0.75 min with a linear increase of 45 °C/min until 140 °C, and standing 1 min at this temperature, followed by a linear increase of 2.5 °C/min until 218 °C, with a further 37 min at 218 °C. For quantification, the molar response factors of Sweet et al. (*15*) were used. The linear velocity of the carrier gas (H_2) was set at 50 cm/s at 218 °C. GC-MS analysis was performed in a HP series 2 gas chromatograph and Trio-1S VG mass-lab with scans between 400 and 35 m/e/s with a 70 eV ionization energy. The chromatographic conditions used were as described for GC-FID. The linear velocity of the carrier gas (He) was set at 40 cm/s at 200 °C, with a solvent delay of 4 min. Methylation analysis was performed in two independent samples from the 1997 harvest and four samples from 1998. The results of the latter were statistically analyzed using the student *t*-test.

NMR Studies. ^1H and ^{13}C NMR spectra were recorded in D_2O on a Bruker Avance 500 spectrometer operating at 500.13 and 125.77 MHz, respectively; the chemical shifts are expressed in δ values relative to sodium trimethylsilyl-2,2,3,3-d_4-propionate (TSS) as external reference. Quantitative ^{13}C NMR spectra were recorded using the inverse gated decoupling sequence, which allows quantitative analysis and comparison of signal intensities, with the following parameters: 4.1 ms pulse width (90° pulse angle); 12 s relaxation delay; 16 K data points; 18 000 scans. The 2D COSYPR (homonuclear shift correlation with presaturation during relaxation delay) spectrum was recorded with 200 transients over 256 increments (zero-filled to 1 K) and 1 K data points with spectral widths of 2000 Hz. The repetition time was 1.5 s. The data were processed in the absolute value mode. The phase-sensitive ^1H-detected (^1H,^{13}C) *g*HSQC (heteronuclear single quantum coherence, using gradient pulses for selection) spectrum was recorded with 200 transients over 256 increments (zero-filled to 1 K) and 1 K data points with spectral widths of 2000 Hz in F_2 and 9000 Hz in F_1. The repetition time was 2.0 s. A cosine multiplication was applied in both dimensions. The delays were adjusted according to a coupling constant ^1J(CH) of 149 Hz. The *g*HMBC (heteronuclear multiple quantum coherence, using gradient pulses for selection) spectrum was recorded with 200 transients over 256 increments (zero-filled to 1 K) and 1 K data points with spectral widths of 2000 Hz in F_2 and 9000 Hz in F_1. The repetition time was 2.0 s. A sine multiplication was applied in both dimensions. The low-pass J-filter of the experiment was adjusted for an average coupling constant ^1J(CH) of 149 Hz and the long-range delay utilized to excite the heteronuclear multiple quantum coherence was optimized for 7 Hz.

RESULTS AND DISCUSSION

NMR Analysis of Fractions sn-CR from Green Olives. NMR spectroscopy was used to obtain structural information about the pectic polysaccharides enmeshed in the cell walls of the olive pulp at the green ripening stage. For that, the sn-CR fractions from green olives of both 1997 and 1998 harvests were used. However, because the spectra were similar, only the results of the 1998 fraction (green sn-CR 1998) are presented.

Correlation $^{13}C-^1H$. **Figure 1** (HSQC spectrum) shows the one-bond correlation of the ^{13}C and the ^1H NMR resonances of this fraction. According to the results described for pectic arabinans from olive pulp cell walls (*7*, *8*), the intense C-1 signals in the spectrum were assigned to the following arabinosyl residues: (1→5)-α-L-Ara*f* and (1→3,5)-α-L-Ara*f* (110.3 ppm), (1→3)-α-L-Ara*f* and T-α-L-Ara*f* (110.0 ppm), and T-*β*-L-Ara*f* (104.3 ppm). These residues are represented in **Figure 2** as residues A−E, respectively. It is important to note that the occurrence of a T-*β*-L-Ara*f* residue has been previously described for pectic arabinans obtained by distinct extraction conditions, from two olive varieties (*8*, *10*). As this terminal residue was presently detected in the pectic fraction enmeshed in the olive pulp cellulosic matrix (sn-CR), the results suggest a highly conserved structural feature of these polysaccharides along the cell walls of the olive fruit. Interestingly, as far as we know, the occurrence of a T-*β*-L-Ara*f* in the arabinan pectic polysaccharides has only been described for the olive pulp cell walls.

On the basis of the sugar composition of fractions sn-CR (*12*) and on literature data (*10*, *16*, *17*), the low-intensity signal at δ_{C-1} = 106.5 was assigned to (1→4)-*β*-D-Gal*p*, whereas the broad signal at δ_{C-1}= 101.8 was assigned to (1→4)-α-D-Gal*p*A. As mentioned by other authors (*18*, *19*), the lower intensity and the broader profile of these signals can occur beause of their scarceness and the lower degree of freedom of the GalA sugar residues when compared to the arabinofuranosyl units.

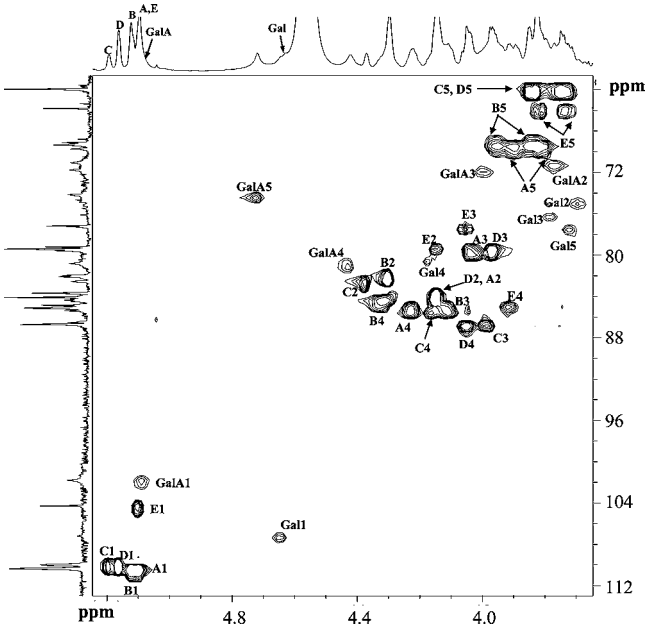

Figure 1. (^{1}H,^{13}C) *g*HSQC spectrum of fraction sn-CR from green olive. Capital letters (A–E) represent the Ara residues according to **Figure 2**. Each number stands for the carbon position giving rise to the cross-peak, according to the chemical shifts given in **Table 1**.

The H-1 signals of the residues were assigned in the HSQC by cross-correlation of the C-1 signals with the H-1 resonances. According to this procedure, the H-1 resonances of residues C, D, and B were attributed to δ_{H-1} = 5.19, 5.16, and 5.12, respectively, and the H-1 resonances of residues A and E were assigned to the signal at δ_{H-1} = 5.10. As previously described for the arabinans from olive pomace (*8*), the identical H-1 resonances of residues A and E allowed us to infer that T-*β*-L-Ara*f* was (1→5)-linked to the arabinan backbone. This conclusion corroborates the hypothesis of a conserved structure for the pectic arabinans in the cell walls of the olive fruit. The HSQC spectrum also showed low-intensity cross-peaks between the C-1 of residues (1→4)-*β*-D-Gal*p* (δ_{C-1} = 106.5) and (1→4)-α-D-Gal*p*A (δ_{C-1} = 101.8) with the H-1 signals at δ_{H-1} = 4.65 and δ_{H-1} = 5.09, respectively.

Correlation $^1H-^1H$. In the COSY spectrum, showing homonuclear ^{1}H−^{1}H correlations (**Figure 3**), it was possible to correlate the H-1 signal of residue C (δ_{H-1} = 5.19) with H-2 (δ_{H-2} = 4.37), H-2 with H-3 (δ_{H-3} = 3.99), H-3 with H-4 (δ_{H-4} = 4.19), and H-4 with H-5 (δ_{H-5} = 3.83 and 3.77). These results and the analysis of the *g*HSQC spectrum allowed us to attribute the resonances of C-2, C-3, C-4, and C-5 of (1→3)-α-L-Ara*f* (residue C) at δ = 82.5, 86.7, 85.4, and 64.0, respectively (**Table 1**). The H-1 signal of residue D (δ_{H-1} = 5.16) was correlated with H-2 (δ_{H-2} = 4.15), H-2 with H-3 (δ_{H-3} = 3.97), H-3 with H-4 (δ_{H-4} = 4.05), and H-4 with H-5 (δ_{H-5} = 3.81 and 3.75). The corresponding resonances of C-2, C-3, C-4, and C-5 were assigned, in the *g*HSQC spectrum, at δ = 84.1, 79.2, 86.7, and 64.0 ppm, respectively. The assignments of H-2, H-3, H-4 and H-5 resonances of the remaining residues were made by a similar procedure. The H-1 signal of the residue B (δ_{H-1} = 5.12) was correlated with H-2 (δ_{H-2} = 4.30 ppm), H-2 with H-3 (δ_{H-3} = 4.11), H-3 with H-4 (δ_{H-4} = 4.31), and H-4 with H-5 (δ_{H-5} = 3.86 and 3.93). The C-2, C-3, and C-4 resonances were identified in the HSQC as δ = 82.1, 85.1, and 84.1, respectively. The existence in this spectrum of multiple signals in the C-5 region at δ_{C-5} = 69.8−68.9 did not allow the exact assignment of C-5 for this residue. At this point, the C-5 resonance of residue B was only tentatively assigned to δ_{C-5} = 69.4. The H-1 signals of residues A and E (δ_{H-1} = 5.10) were both correlated with H-2 at δ_{H-2} = 4.15, but distinct H-3 (δ = 4.05 and 4.02), H-4 (δ = 4.22 and 3.91), and H-5 (δ = 3.90, 3.80, and 3.73) were respectively obtained for these residues. The specific attribution of H-3, H-4, and H-5 resonances of residues A and E was supported by comparison of their related C-3, C-4, and C-5 resonances to those reported by other authors (*10*, *20*). The C-2, C-3, C-4, and C-5 resonances of residue A were attributed in the HSQC to δ = 83.7, 79.4, 85.1, and 69.4 (only tentatively), respectively, and those of residue E were assigned to δ = 79.2, 77.2, 84.9, and 65.9. It should be noted that the chemical shifts reported for the arabinofuranosyl units were similar to the ones described by Cardoso et al. (*8*), except the swap of H-5 and C-5 of residues A and B. The present assignments are in accordance with those reported by Dourado et al. (*18*), also based on the COSY and HSQC spectra, allowing us to infer that those previously reported by Cardoso et al. (*8*), tentatively assigned on the basis of literature data, were not correct. Besides the correlation peaks for the arabinofuranosyl units, the COSY spectrum showed low intense correlation cross-peaks between H-1 and H-2 of residues (1→4)-*β*-D-Gal*p* (δ_{H-2} = 3.72) and (1→4)-α-D-GalA*p* (δ_{H-2} = 3.77), allowing the assignment of their C-2 resonance, in the HSQC, at δ = 74.8 and 71.1, respectively. Because the correlations for the remaining protons of these residues were not observed in the COSY spectrum, some of their proton resonances were alternatively assigned in the HSQC spectrum (values in **Table 1**), after identification of their carbon resonances according to the literature data (*10*, *16*, *17*).

Long-Distance Correlation $^{13}C-^1H$. The analysis of the HMBC spectrum (**Figure 4**) that shows long-range ^{13}C−^{1}H correlations (two and three bonds distance) gave additional information about the structure of the pectic arabinans. For simplification, only the new interpreted cross-peaks are shown in this figure. It was possible to observe a cross-peak between δ_{H-5} = 3.93 of residue B with the anomeric carbon of residue E ($\delta_{C\ 1}$= 104.3), showing that the T-*β*-Ara*f* was linked to a (1→3,5)-Ara*f* residue. It is worth noting that a similar cross correlation peak was described by Cardoso et al. (*8*). However, because of the swap on the H-5 assignment of residues A and B, the previous tentative attribution should not be considered.

The HMBC spectrum also showed multiple correlation peaks between the C-5 signals of residues A and B with their H-3, suggesting that these residues can have different environments on the pectic arabinan side chains. In particular, residue A showed cross-correlations between its H-3 (δ_{H-3} 4.05−3.99) and C-5 resonances at δ_{C-5} = 69.2, 69.4, and 69.8. For residue B, cross-correlations were observed between the H-3 (δ_{H-3} = 4.11−4.08) and two distinct C-5 signals (δ_{C-5} = 68.9 and 69.4). These results allowed the conclusive attributions of H-3 and C-5 resonances of residues A and B (**Table 1**), and the proposal of the occurrence of branched and linear blocks in the arabinan backbone (**Figure 2**), as this would originate different environments in residues A and B. Moreover, the HMBC shown in **Figure 4** is similar to that obtained for the arabinans of pectic polysaccharides of the olive pomace (*8*); in particular, the multiple cross-correlations of H-3 and C-5 were also evident in the HMBC spectrum obtained by Cardoso et al. (*8*) for those polysaccharides, although not interpreted by the authors at the time. On the basis of the present and previous results (*8*), we propose a more representative tentative structure for olive pulp arabinans in **Figure 2**. Once more, these results support the presence of a highly preserved structure for the arabinans of

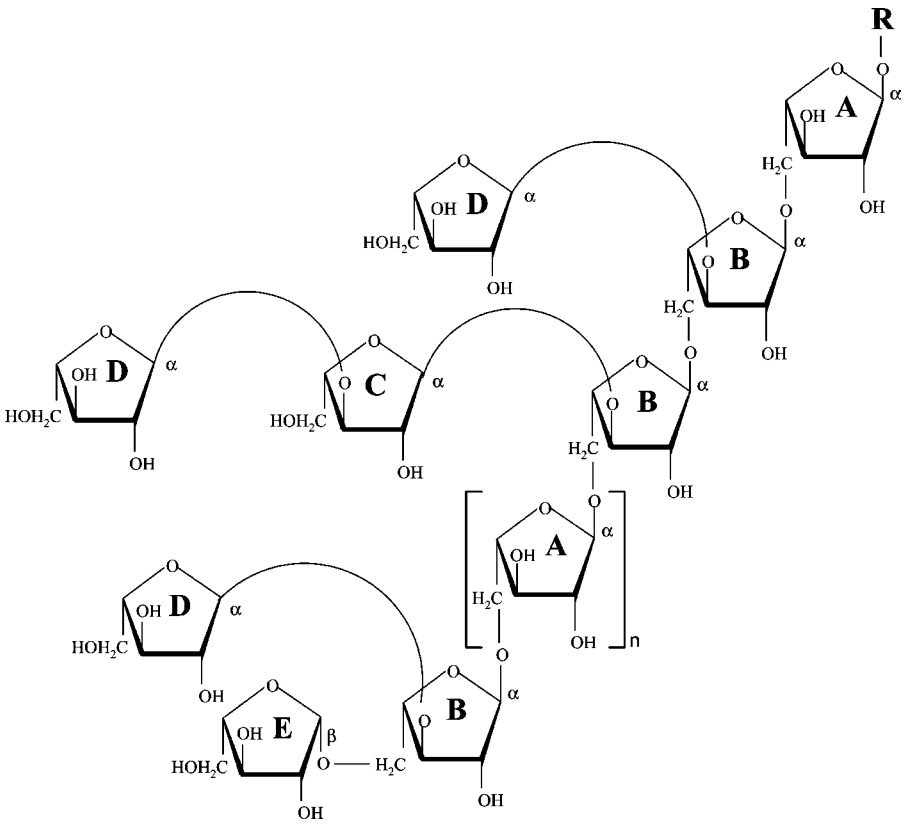

Figure 2. Proposed structure for the arabinan moiety of the pectic polysaccharides of fraction sn-CR from green olive.

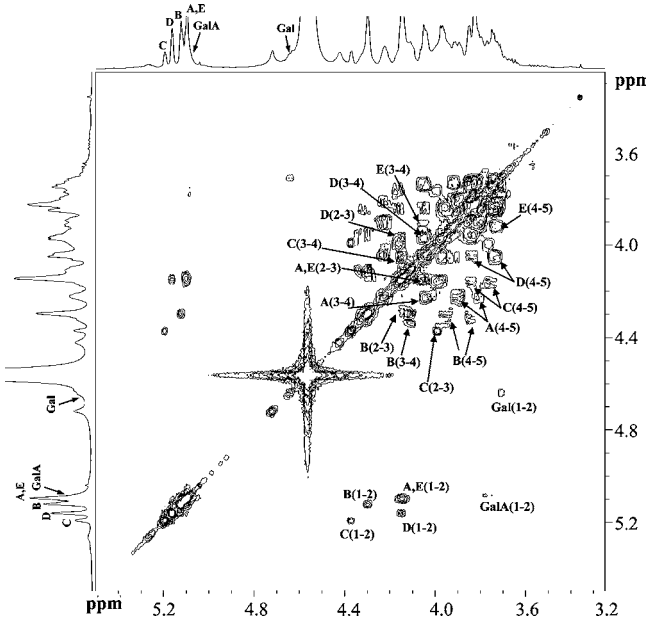

Figure 3. 2D COSYPR spectrum of the green sn-CR fraction. Capital letters (A–E) represent the Ara residues according to **Figure 2**. The numbers in parentheses denote the hydrogen atoms attached to the given carbons.

the pectic polysaccharides along all the cell walls of the olive fruit.

Methylation Analysis of sn-CR Fractions from Olive Pulp at Different Ripening Stages. Methylation analysis was used to confirm the sugar residue assignments in the NMR studies and to evaluate the ripening-related changes of the pectic arabinans. In this assay, special attention was paid to the arabinosyl and the rhamnosyl-linkage composition of the samples, as they are, respectively, the mainly sugar components of the arabinans and their anchorage point to the main chain of the rhamonogalacturonan backbone of the pectic polysaccharides. (1→5)-Ara*f*, T-Ara*f*, (1→3,5)-Ara*f*, and (1→3)-Ara*f* arabinosyl linkages were identified (**Table 2**) that corresponded to all the arabinosyl residues observed in the NMR spectra. Concerning the rhamnosyl units, only (1→2)-Rha*p* and (1→2,4)-Rha*p* were detected in the sn-CR fractions by methylation analysis. **Table 2** shows the (1→2,4)-Rha*p*/Total Rha*p* ratio for fractions sn-CR obtained from two harvest years (1997 and 1998) at green, cherry, and black ripening stages. The ratios were higher in 1998 (0.58−0.70) than in 1997 (0.44−0.60), showing that, on average, the degree of branching of the pectic polysaccharides in fractions sn-CR from 1997 was higher. Considering the (1→2,4)-Rha*p*/Total Rha*p* mean ratio for both years, the pectic polysaccharides of green and cherry olives had approximately one branched Rha*p* residue for every two, whereas this ratio was increased to approximately two in three in the black olives. These results suggested that the pectic polysaccharides held in the cellulosic matrix of the black olives were, on average, more branched than those held in the green and cherry olives. Their solubilization to the sn-CR fraction was probably due to the loss of the integrity and firmness of the cell wall (*1*). Alternatively, the greater degree of branching of the sn-CR fraction from black olives can be due to the biosynthesis of highly branched pectic polysaccharides in the ripe black olives, as suggested by Mafra et al. (*2*).

The influence of the olive ripening on the degree of polymerization (DP) of the pectic arabinans in fraction sn-CR was estimated by the total Ara*f*/(1→2,4)-Rha*p* ratio. As can be seen in **Table 2**, this ratio was diminished for riper olives, with the greater decrease occurring from cherry (82 and 77) to black olives (36 and 46) for 1997 and 1998, respectively. These results suggest that the pectic arabinans highly entrapped in the cell

Table 1. ^{1}H and ^{13}C NMR Chemical Shifts (δ) of the Arabinan-Rich Pectic Polysaccharides (Fraction sn-CR) from Green Olive Pulp

		chemical shift (δ)					
		1	2	3	4	5	6
				Arabinofuranosyl Residues			
A: (1→5)-α-Ara*f*	^{1}H	5.10[b]	4.15[c]	4.05–3.99[c,d]	4.22[c]	3.90/3.80[c]	
	^{13}C	110.3[a]	83.7[b]	79.4[b]	85.1[b]	69.2/69.4/69.8[b,d]	
B: (1→3,5)-α-Ara*f*	^{1}H	5.12[b]	4.30[c]	4.11–4.08[c,d]	4.31[c]	3.93/3.86[c]	
	^{13}C	110.3[a]	82.1[b]	85.1[b]	84.1[b]	68.9/69.4[b,d]	
C: (1→3)-α-Ara*f*	^{1}H	5.19[b]	4.37[c]	3.99[c]	4.19[c]	3.83/3.77[c]	
	^{13}C	110.0[a]	82.5[b]	86.7[b]	85.4[b]	64.0[b]	
D: T-α-Ara*f*	^{1}H	5.16[b]	4.15[c]	3.97[c]	4.05[c]	3.81/3.75[c]	
	^{13}C	110.0[a]	84.1[b]	79.2[b]	86.7[b]	64.0[b]	
E: T-β-Ara*f*	^{1}H	5.10[b]	4.15[c]	4.02[c]	3.91[c]	3.73[c]	
	^{13}C	104.3[a]	79.2[b]	77.2[b]	84.9[b]	65.9[b]	
				Galacturonosyl Residues			
(1→4)-α-Gal*p*A	^{1}H	5.09[b]	3.77[c]	4.02[b]	4.42[b]	4.72[b]	ni
	^{13}C	101.8[e]	71.1[b]	71.8[e]	79.7[e]	74.2[e]	173.0[e]
				Galactosyl Residues			
(1→4)-β-Gal*p*	^{1}H	4.65[b]	3.72[c]	3.79[b]	4.18[b]	3.74[b]	ni
	^{13}C	106.5[b]	74.8[b]	76.2[e]	79.3[e]	77.3[e]	ni

[a] Assignments from ^{13}C spectrum in accordance with the sugar residues obtained by methylation analysis. [b] Assignments from HSQC spectrum. [c] Assignments from COSY spectrum. [d] Assignments from HMBC spectrum. [e] Assignments based on literature data; ni = not identified.

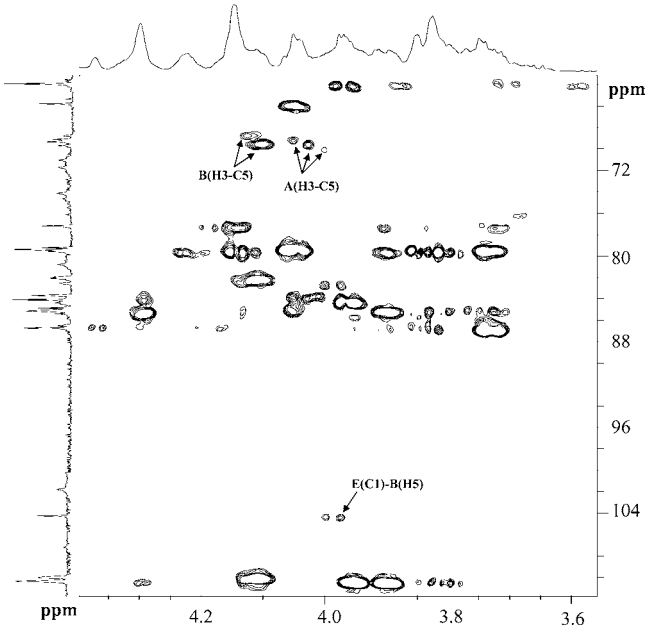

Figure 4. Expansion of the (^{1}H,^{13}C) *g*HMBC spectrum of fraction sn-CR from green olive. Capital letters represent the Ara residues according to **Figure 2**.

walls of black olives must be shorter in comparison with the pectic arabinans from the green and cherry olives.

To clarify the structural ripening-related changes of the arabinans of these pectic polysaccharides, we estimated the relative amount of the different arabinosyl sugar residues for the three sn-CR fractions of both harvest years (**Table 2**). Considering the harvest year of 1997, the arabinosyl-linkage composition for T-Ara*f*, (1→5)-Ara*f*, (1→3)-Ara*f*, and (1→3,5)-Ara*f* was similar for green and cherry olives (approximately 2.1:2.9:1.0:1.6 and 1.8:2.9:1.0:1.4, respectively). In black olives, pectic arabinans of fraction sn-CR were considerably richer in T-Ara*f* and (1→3,5)-Ara*f* and poorer in (1→5)-Ara*f* and (1→3)-Ara*f*. At this ripening stage, the relative proportion found for the arabinofuranosyl residues was 4.0:2.9:1.0:3.8. sn-CR fraction from green and cherry olives from 1998 had distinct arabinosyl-linkage composition, with the green fraction having more branching residues than the cherry stage. However, as for 1997, an increase in T-Ara*f* and (1→3,5)-Ara*f*, and a decrease in (1→5)-Ara*f* and (1→3)-Ara*f* residues were observed between the cherry (relative arabinosyl composition of 1.9:3.1:1.0:1.6) and the black ripening stages, with the pectic arabinans of the black olives containing the same arabinosyl composition of those of 1997. Considering the relative amount of (1→3,5)-Ara*f* residues in the two harvest years, it can be inferred that the pectic arabinans in fraction sn-CR from cherry olives had, as a mean value, one branching point per each 4 residues, whereas those in black olive had, as a mean value, one branching point per each 2 Ara*f* residues. Also, attending to the (1→3)-Ara*f*/(1→5)-Ara*f* ratio, it is possible to infer that the arabinans from black and cherry olives had, respectively, one and two (1→3)-Ara*f* per three branching points. Thus, the methylation analysis allowed us to conclude that the pectic polysaccharides deeply enmeshed in the cell walls of black olives have more arabinan side chains than those found in the cherry olives. Also, these arabinans are shorter (fewer (1→5)-Ara*f*), and highly branched (more (1→3,5)-Ara*f*) with short side chains (fewer (1→3)-Ara*f*). Once more, the distinct reported features in the structure of the pectic polysaccharides from the green, cherry, and black olives can suggest structural modification or, alternatively, synthesis of new pectic polysaccharides.

Quantitative ^{13}C NMR Analysis of sn-CR Fractions from Olive Pulp at Different Ripening Stages. Quantitative ^{13}C NMR was registered for all the pectic sn-CR extracts (**Figure 5**), and the relative amount of (1→5)-α-L-Ara*f* plus (1→3,5)-α-L-Ara*f*, (1→3)-α-L-Ara*f* plus T-α-L-Ara*f*, and T-β-L-Ara*f* (**Table 3**) was estimated after integration of the corresponding area of their C-1 signals at δ_{C-1} = 110.3, 110.0, and 104.3, respectively. In general, the relative amount of the T-β-L-Ara*f* in the pectic arabinans was decreased by the olive ripening, for both harvest years. This effect was mostly evident in the olives harvested in 1997, which showed a decrease in the relative amount of that residue for all the ripening stages, and in particular, from cherry to black stages (**Figure 5** and **Table 3**). Also, for these two ripening stages, comparable results could be found for the relative amount of the arabinosyl residues quantified by the ^{13}C NMR and those estimated by the methylation analysis (**Tables 2** and **3**). Considering the harvest year of 1998, sn-CR fractions from green and cherry olives

Table 2. Molar Ratios ((1→2,4)-Rha*p*/Total Rha*p* and Total Ara*f*/(1→2,4)-Rha*p*) and Arabinosyl-Linkage Composition of sn-CR Fractions Obtained by Methylation Analysis from Olive Pulp in Two Harvests and at Three Ripening Stages; For Each Row, Means with the Same Letter Are Not Significantly ($p > 0.05$) Different ($n = 4$) and Values within Parentheses Are the Coefficients of Variation

	1997			1998		
	green	cherry	black	green	cherry	black
			Molar Ratio			
(1→2,4)-Rha*p*/Total Rha*p*	0.44	0.45	0.60	0.60 (9) a	0.58 (3) b	0.70 (4) a
Total Ara*f*/(1→2,4)-Rha*p*	93	82	36	84 (5) a	77 (3) a	46 (4) b
			Arabinosyl-Linkage Composition (mol %)			
T-Ara*f*	28	25	36	35 (2) a	25 (2) b	36 (3) a
(1→5)-Ara*f*	38	41	26	26 (4) a	41 (2) b	26 (7) a
(1→3)- Ara*f*	13	14	9	9 (3) a	13 (6) b	9 (2) a
(1→3,5)-Ara*f*	21	20	30	29 (1) a	21 (2) b	30 (3) a

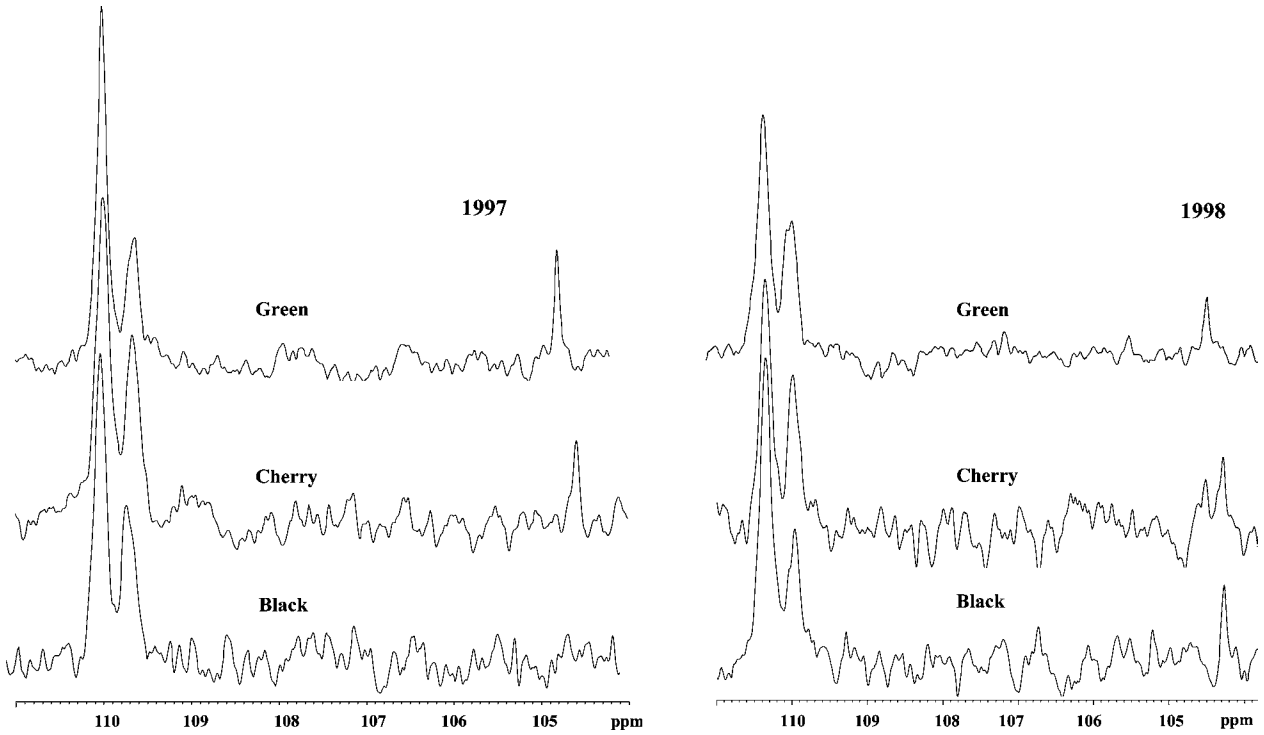

Figure 5. Quantitative ^{13}C NMR spectra of sn-CR fractions obtained from olive pulp in two harvests and at three ripening stages.

Table 3. Relative Arabinosyl Composition of sn-CR Fractions Obtained by Quantitative ^{13}C NMR Spectra from Olive Pulp in Two Harvests and at Three Ripening Stages

sample	(1→5)-α-Ara*f* (1→3,5)-α-Ara*f*	T-α-Ara*f* (1→ 3)-α-Ara*f*	T-β-Ara*f*
	1997		
green	46	45	9
cherry	60	33	7
black	59	37	<3
	1998		
green	56	35	9
cherry	58	33	9
black	48	47	5

showed similar relative amounts of T-β-L-Ara*f* (9%), but a decrease in this residue was also observed from cherry to black stages. These distinct quantitative ^{13}C NMR data from the 1997 and 1998 green and cherry samples confirmed the results of Mafra et al. (*2*), showing that the samples of 1998 harvest, although presenting green, cherry, and black colors, had less-distinct ripening characteristics than those of 1997. However, opposite to the results described for those authors, the disappearance of the T-β-L-Ara*f* residue in the arabinans structure along the olive ripening suggests that structural modification was occurring, superimposing the de novo synthesis of these arabinan structures.

In conclusion, the 1D and 2D NMR spectroscopy analysis of arabinan rich pectic extracts from the cellulosic residue of two consecutive harvests at the green ripening stage allowed us to report, for the first time, the main structural features of the arabinans of the pectic polysaccharides highly entangled in the olive pulp cellulosic matrix (sn-CR). As these arabinans have the same general characteristics than those obtained with mild extraction processes, a highly conserved structural feature was proposed for these polysaccharides all along the cell walls of the olive fruit.

Ripening of the olives induces structure modifications in the pectic polysaccharides deeply enmeshed in the cell walls. Black olives have more and shorter arabinan side chains, highly branched, and with shorter side chains than those of green and cherry olives. These modifications involved the cutting of the characteristic terminally linked β-Ara*f* residue of the arabinans. This odd feature can be used as a diagnostic tool in the evaluation of the stage of ripening of this fruit, as well as a marker of authenticity for the presence of olive pulp in matrices containing pectic polysaccharides samples.

ABBREVIATIONS USED

CWM, cell wall material; NMR, nuclear magnetic resonance; HSQC, heteronuclear single quantum correlation; COSY, homonuclear correlation spectroscopy; HMBC, heteronuclear multiple bond correlation; GC-FID, gas chromatography coupled to a flame ionization detector; GC/MS, gas chromatography/mass spectrometry; sn-CR, supernatant from the dialysis of the cellulosic residue.

LITERATURE CITED

(1) Mafra, I.; Lanza, B.; Reis, A.; Marsilio, V.; Campestre, C.; Angelis, M.; Coimbra, M. A. Effect of ripening on texture, microstructure and cell wall polysaccharide composition of olive fruit. *Physiol. Plant.* **2001**, *111*, 439−447.

(2) Mafra, I.; Barros, A. S.; Nunes, C.; Vitorino, R.; Saraiva, J.; Smith, A.; Waldron, K. W.; Delgadillo, I.; Coimbra, M. A. Ripening-related changes in the cell walls of olive pulp (*Olea europaea* L.) of two consecutive harvests. *J. Sci. Food Agric.* **2006**, *86*, 988−998.

(3) Huisman, M. M. H.; Schols, H. A.; Voragen, A. G. J.; Changes in cell wall polysaccharides from ripening olive fruits. *Carbohydr. Polym.* **1996**, *31*, 123−133.

(4) Vierhuis, E.; Schols, H. A.; Beldman, G.; Voragen, A. G. J. Isolation and characterisation of cell wall material from olive fruit (*Olea europaea* cv koroneiki) at different ripening stages. *Carbohydr. Polym.* **2000**, *43*, 11−21.

(5) Jiménez, A.; Rodríguez, R.; Fernández-Caro, I.; Guillén, R.; Fernández-Bolãnos, J.; Heredia, A. Olive fruit cell wall: degradation of pectic polysaccharides during ripening. *J. Agric. Food Chem.* **2001**, *49*, 409−415.

(6) Fernández-Bolanos, J.; Rodríguez, R.; Guillén, R.; Jiménez, A.; Heredia, A. Activity of cell wall-associated enzymes in ripening olive fruit. *Physiol. Plant.* **1995**, *93*, 651−658.

(7) Coimbra, M. A.; Waldron, K. W.; Selvendran, R. R. Isolation and characterisation of cell wall polymers from olive pulp (*Olea europaea* L.). *Carbohydr. Res.* **1994**, *252*, 245−262.

(8) Cardoso, S. M.; Silva, A. M. S.; Coimbra, M. A. Structural characterisation of the olive pomace pectic polysaccharide arabinan side chains. *Carbohydr. Res.* **2002**, *337*, 917−924.

(9) Renard, C. M. G. C.; Voragen, A. G. J.; Thibault, J. F.; Pilnik, W. Studies on apple protopectin. 5. Structural studies on enzymatically extracted pectins. *Carbohydr. Polym.* **1991**, *16*, 137−154.

(10) Coimbra, M. A.; Delgadillo, I.; Waldron, K. W.; Selvendran, R. R. Isolation and Analysis of Cell Wall Polymers from Olive Pulp. In Linskens, H.-F., Jackson, J. F., Eds.; *Modern Methods of Plant Analysis*; Springer-Verlag: Berlin, 1996; Vol. 17, pp 19−44.

(11) Selvendran, R. R.; Ryden, P. Isolation and analysis of plant cell walls. In Dey, P. M., Ed.; *Methods in Plant Biochemistry*; Academic Press: London, 1990; Vol. 2, pp 549−579.

(12) Ferreira, J. A.; Mafra, I.; Soares, M. R.; Evtuguin, D. V.; Coimbra, M. A. Dimeric calcium complexes of arabinan-rich pectic polysaccharides from *Olea europaea* L. cell walls. *Carbohydr. Polym.* **2006**, *65*, 535−543.

(13) Ciucanu, I.; Kerek, F. A simple and rapid method for permethylation of carbohydrates. *Carbohydr. Res.* **1984**, *131*, 209−217.

(14) Isogai, A.; Ishizu, A.; Nakano, J. A new facile methylation method for cell-wall polysaccharides. *Carbohydr. Res.* **1985**, *138*, 99−108.

(15) Sweet, D. P.; Shapiro, R. H.; Albersheim, P. Quantitative analysis by various G. L. C. response-factor theories for partially methylated and partially ethylated alditol acetates. *Carbohydr. Res.* **1975**, *40*, 217−225.

(16) Habibi, Y.; Heyraud, A.; Mahrouz, M.; Vignon, M. R. Structural features of pectic polysaccharides from the skin of *Opuntia ficus-indica* prickly pear fruits. *Carbohydr. Res.* **2004**, *339*, 1119−1127.

(17) Navarro, D. A.; Cerezo, A. S.; Stortz, C. A. NMR spectroscopy and chemical studies of an arabinan-rich system from the endosperm of the seed of *Gleditsia triacanthos*. *Carbohydr. Res.* **2000**, *337*, 255−263.

(18) Dourado, F.; Cardoso, S. M.; Silva, A. M. S.; Gama, F. M.; Coimbra, M. A. NMR structural elucidation of the arabinan from *Prunus dulcis* immunobiological active pectic polysaccharides. *Carbohydr. Polym.* **2006**, *66*, 27−33.

(19) Schols, H. A.; Posthumus, M. A.; Voragen, A. G. J. Hairy (ramified) regions of pectins. 1. Structural features of hairy regions of pectins isolated from apple juice produced by the liquefaction process. *Carbohydr. Res.* **1990**, *206*, 117−129.

(20) Akiyama, Y.; Mori, M.; Kato, K. C-13 NMR analysis of Hydroxyproline arabinosides from Nicotiana tabacum. *Agric. Biol. Chem.* **1980**, *44*, 2487−2489.

Received for review March 15, 2007. Revised manuscript received May 29, 2007. Accepted June 14, 2007. We are grateful for the financial support of the EU Project OLITEXT FAIR CT97-3053 and FCT for funding the Research Unit 62/94 "Química Orgânica, Produtos Naturais e Agro-Alimentares".

JF070769W